

PRACTICAL ISSUES ON THE MODELING OF PERMANENT-MAGNET MACHINES AND COGGING TORQUE CALCULATIONS IN TWO-DIMENSIONAL FINITE-ELEMENT ANALYSIS

Antônio Flavio Licarião Nogueira¹

¹Universidade do Estado de Santa Catarina, Joinville, Brazil

ABSTRACT

The paper contains a description of practical issues that should be considered during the planning of finite element models. The given examples concern a direct current (*dc*) motor with surface-mounted permanent magnet rotor. Two techniques for simulation of the rotor movement are described, and the necessary steps to specify the directions of magnetization of both isotropic and nonisotropic curved permanent magnets are highlighted. The concept of torque pulsations is introduced. Upon this, the procedure to determine the cogging torque characteristic numerically is explained and the resulting curve is exhibited.

Keywords: *Boundary conditions, Cogging torque, Finite element analysis, Permanent magnets*

1. INTRODUCTION

When dealing with problems that involve complex geometries, it is very important to plan the finite element model, especially in its aspects concerned with mesh construction and specification of the boundary conditions. This will allow extra flexibility for altering material properties, defining sequences of similar problems and facilitates the analysis of the results. Some of the practical issues usually considered during the planning of the finite element models are:

- Percentage of the entire structure to be examined;
- Displacement of movable parts;
- Fineness of the mesh in some millimetric gaps, pole tips and reentrant corners;
- Identification of repetitive portions.

These points are now discussed as they are applied to the numerical modeling of a direct current (*dc*) motor. A cross-sectional view of the motor is shown in figure 1. The motor contains radially oriented neodymium-iron-boron permanent magnets to provide a four-pole rotor excitation. Each magnet arc spans 50 mechanical degrees, and the stator has 36 evenly spaced slots. The air-gap length between the outer periphery of the magnets and the inner radius of the stator is 2.0 mm. The depth of the laminated stack in the longitudinal or *z*-direction is 7.6 cm. Regions of prime interest for the construction of the model are indicated in the illustration of figure 2.

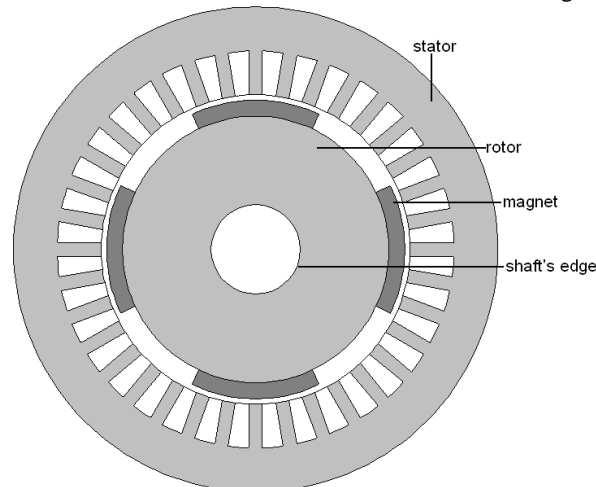


Figure 1. Cross-sectional view of a *dc* surface-mounted permanent-magnet motor.

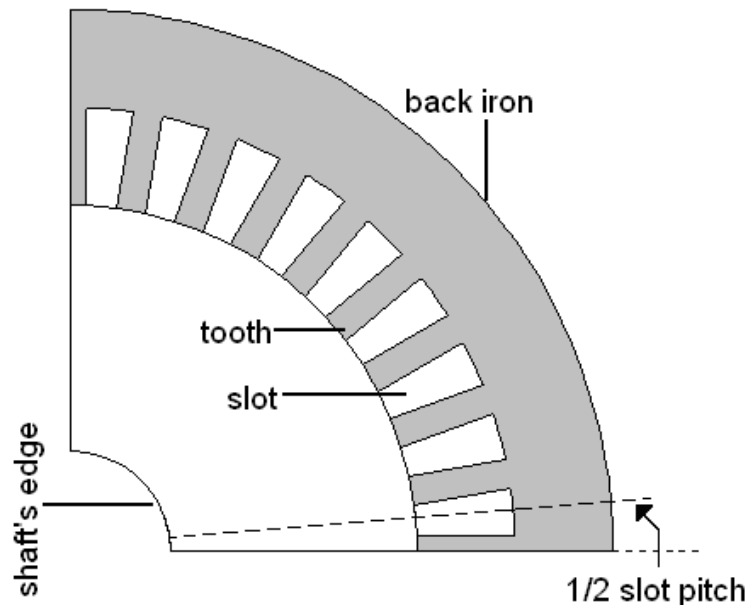


Figure 2. Regions for the construction of the model.

2. LITERATURE REVIEW

The modeling of electrical machines is focused on several scientific publications that describe analytical and numerical models used to simulate the behaviour of motor devices and reach optimized designs [1], [2]. Electromagnetic CAD systems based on the finite element technique are widely used in industry and research establishments to predict the field distribution of a given device, as well as several design parameters, with high accuracy. To better illustrate the practical issues on the planning of two-dimensional finite-element models, the problem of evaluating the cogging torque in permanent-magnet machines is now considered.

The calculation of cogging torques in permanent-magnet machines is a notoriously difficult task, and the subject has been investigated by many researchers [3]. A great number of permanent-magnet motors are manufactured for use in industrial robots, numerically controlled machines and computer peripherals. The performance of these machines is adversely affected by torque pulsations such as *cogging* and *commutation torques*. The combination of cogging torque and torque ripple results in undesired vibration and noise during machine operation, and there have appeared many ways to reduce cogging torque in electric machines [4], [5]. Cogging torque minimization is specially important in applications such as high performance speed control and positioning systems, permanent-magnet synchronous motors for electric vehicles [6] and permanent-magnet generators for wind power applications [7]. In principle, this torque can be reduced, or even eliminated, by twisting the rotor (or stator) stack or the magnets, and this process is known as “skewing”. Alternatively, cogging torques can be reduced to acceptable levels by appropriate selection of some dimensions, such as pole face width and slot opening [8], [9], [10].

Accurate prediction of cogging torque is carried out with substantial difficulties. Cogging torque characteristics are functions of the rotor angular position and these functions are, in most cases, periodic. The period usually represents a small percent of a complete revolution. In most practical motors, this period is equal to one slot pitch. To compute the cogging torque, it is necessary to simulate incremental motion of the rotor, and this requires at least one field solution for each rotor position. The different rotor positions are separated by a fraction of a slot pitch, and this means positional displacements that are typically one mechanical degree or less. Clearly, the changes in the machine’s magnetic field resulting from such fractional rotations are small, and so are the changes in the magnetic stored energy and local stresses.

Computation of cogging torques has received considerable attention in the literature since the decade of 1970 [11]. Analytical models for predicting the cogging torque of permanent-magnet motors usually provide equations for calculating the cogging torque in terms of the air-gap normal flux density and geometrical dimensions of the machine. Additionally, some of these analytical methods incorporate the effect of skewing and the resulting equations can be programmed and used for parametric studies and shape optimization [12], [13].

Most reported cogging torque computations are based on the traditional force and torque calculation methods of virtual work and Maxwell stress tensor. The method of mean and difference potentials has also been applied to the calculation of cogging torques in permanent-magnet motors [14]. This technique avoids numerical differentiation

entirely and reported results on cogging torque prediction agree with measured values within the limits of measurement accuracy and the approximations inherent to a two-dimensional analysis [3], [15].

3. PRACTICAL ISSUES ON MODELING

3.1. Inspection of the device's symmetry

The analysis of the entire structure is computationally expensive, and a great deal of time can be saved by analyzing only a part of the structure. In this case, however, it is very important to conduct a preliminary inspection to ensure correct specification of boundary conditions. For electrical machines, the analysis can be performed using only one pole-pitch because the boundary conditions can be readily identified for such a problem [16]. These usually consist of, firstly, enforcing a flux-line boundary along the shaft edge and along the outer periphery of the machine and, secondly, specifying anti-periodicity conditions for the two lateral edges separated by one pole pitch. See figure 3. In the illustration of figure 3, the two bounding radial lines are drawn exactly one pole pitch apart. The magnetic vector potential A at a given radial position r on one line will be exactly the negative of the vector potential at the corresponding radial position on the other, i.e.

$$A(r, \theta) = -A(r, \theta + \pi/2). \tag{1}$$

To specify anti-periodic boundary conditions for the model shown in figure 3, it is necessary to create four distinct boundary properties [17]. These properties will link together faces 1 and 1', 2 and 2', 3 and 3', 4 and 4'.

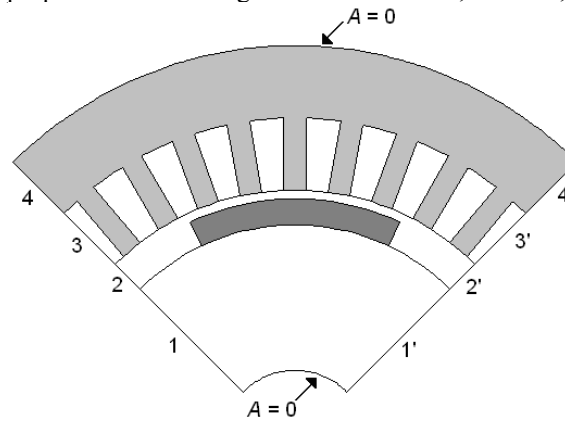


Figure 3. Boundary conditions for a four-pole dc motor.

In the case of an electric machine, it is not even necessary the model to be bounded by radial lines. The model shown in figure 4 represents a 10° rotation of the rotor in the counter-clockwise direction. The same four boundary properties used to define anti-periodic boundary conditions in the model shown in figure 3 can be used to link together the faces of the two new lateral boundaries. It is worth noting that in the model shown in figure 4, faces 2 and 2' continue to be exactly one pole pitch apart, that is, 90 mechanical degrees.

It is always convenient to have the model symmetrically displaced with respect to the origin of the coordinate axes. This facilitates not only the input of geometrical coordinates but also the specification of the direction of remanence of existing permanent magnets.

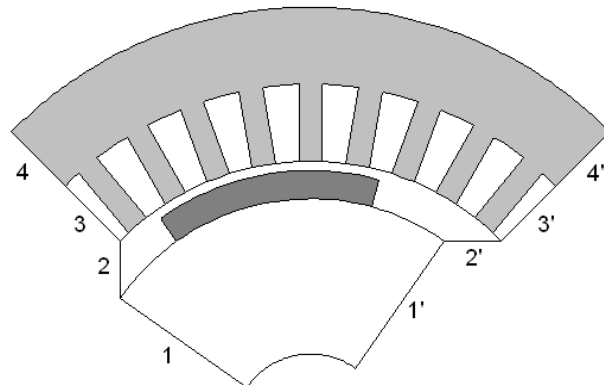


Figure 4. Field problem that represents a 10° rotation of the rotor in the counter-clockwise direction.

3.2. Slip plane

The slip plane is an arc placed in the mean gap and, sometimes it is required this arc to contain equally spaced nodes. When modeling electrical machines, it is possible to build two main models: one for the rotor, other for the stator, and the slip plane may be taken as an artificial interface between the models. Each of the two models may include a fraction of the air-gap region, to avoid the construction of a separate model only for this region; the model for the stator, for example, may, additionally include the portion of the air-gap region situated between the slip plane and the inner radius of the stator teeth.

The concept of slip plane is very useful in simulating rotating devices. As well as facilitating the joining of separate models, it allows the implementation of correct mesh deformation, caused by displacement of movable parts, without causing mismatched nodes.

3.3. Elementary cells

The mesh around the corners of the stator teeth needs an extra degree of fineness. This is in order to minimize the effect of the numerical singularity existent at these corners. The geometric periodicity of the stator teeth, however, may be exploited in a way that the meshing effort of these critical regions is concentrated on the proper discretization of an elementary model. Later, this cell can be readily replicated to form the full stator region model. An elementary model or cell that spans half a slot pitch is adequate for the initial construction of the mesh. In the circumferential direction, the model is internally bound by the slip plane and externally by the motor outer periphery. In the radial direction, it is bound by two radial lines, one coinciding with the centre of a tooth, the other coinciding with the centre of a slot.

The drawing of an outline representing half a tooth, part of the back iron and one half of a slot is carried out by entering a few key points, and defining the necessary primitives consisting of straight lines and arcs. This is illustrated in figure 5. The node density around the tooth corner can be increased by further subdividing the primitives that intersect at the tooth tip. Further alterations of the mesh can be carried out, by increasing the number of subdivisions of the faces or by inserting new nodes and defining new regions.

It is very important to check that the discretization of the elementary model is satisfactory, and that the number of nodes and elements already defined is not too large, before moving to the stage where the whole stator is modeled. If, for example, second-order triangular finite elements are going to be used in future analyses, the number of nodes will be almost quadruplicated.

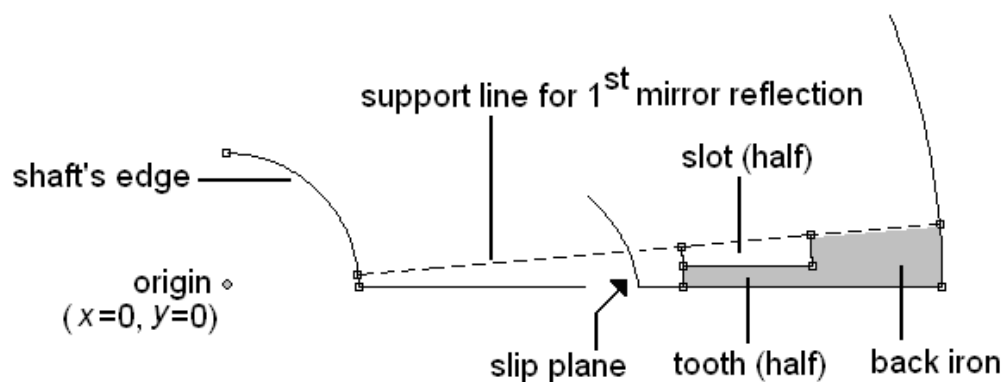


Figure 5. Elementary cell for the stator.

3.4. Model for the stator

A full stator model can be created by replicating the elementary model. The sequence consists of coordinate transformations such as mirror reflections through specified line segments. The areas accommodating the conductors in the slots are better represented by distinguished regions in order to allow the specification of distinct values of the drive currents in different slots.

3.5. Model for the rotor

The main feature of the model built for the rotor is the specification of the permanent magnets' properties. A useful documentation on the different ways to specify the directions of magnetization of machines with arc-shaped magnets may be found in [18]. There exist curved magnets that are either, magnetized in a set direction or magnetized radially. In the illustration of figure 6, the magnets are isotropic and magnetized in a set direction. The

arrows in figure 6 indicate that magnetic flux emerges from the outer surface of magnets “1” and “3” (north poles), and enters the outer surfaces of magnets “2” and “4” (south poles). For each magnet, it is indicated the angle, in degree, for the direction of magnetization attributed to the whole area – or volume – occupied by the permanent magnet.

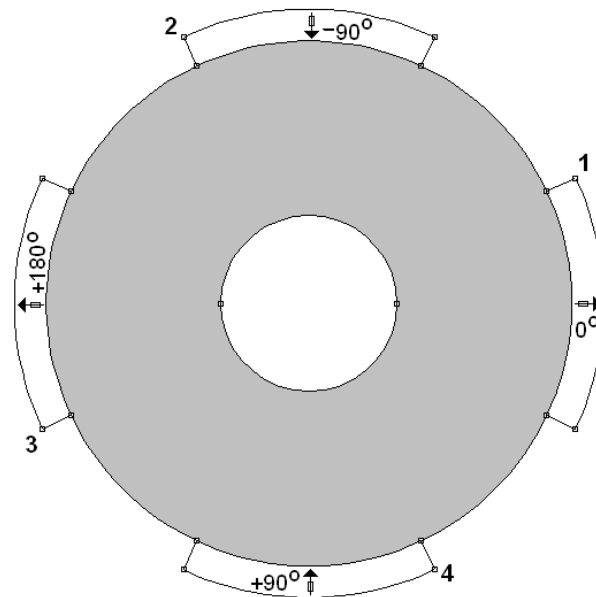


Figure 6. Permanent magnets 1, 2, 3 and 4 magnetized in a set direction.

As the rotor moves, it is necessary to redefine the magnetization directions of the permanent magnets. This redefinition is easily performed when the movement is simulated using the technique of mesh distortion discussed in a later section. To simulate a rotor movement of one degree in the counter-clockwise direction, for example, the magnetization directions of the permanent magnets that appear in figure 6 should be specified according to the directions indicated in the illustration of figure 7.

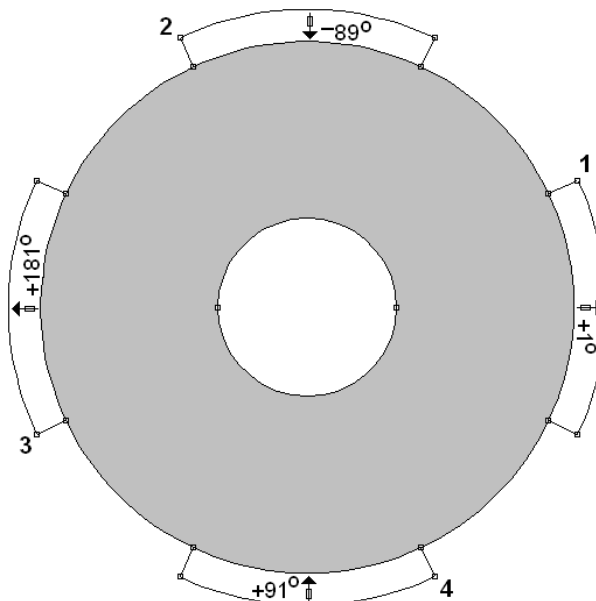


Figure 7. Redefinition of magnetization directions for magnets 1, 2, 3 and 4.

For nonisotropic radially-oriented permanent magnets, one may define a number of adjacent sectors or regions, all distinguished by a different label, in order to specify the different directions of magnetization. In the circumferential direction, each sector is bound by two arcs, and the internal arc is attached to the outer surface of the round rotor. In the radial direction, each sector is bound by two lateral edges.

The permanent magnet illustrated in figure 8 spans 50 mechanical degrees and represents a north pole. In this approximation, the angle of separation between the lateral edges is 10 mechanical degrees, and the angles in degree of the radial lines that bound the individual sectors are indicated in brackets. For each sector, the direction of magnetization that points outwards from the origin is approximated by the mean value of the two angles of the bounding radial lines. These values are indicated outside the individual sectors *a*, *b*, *c*, *d* and *e*.

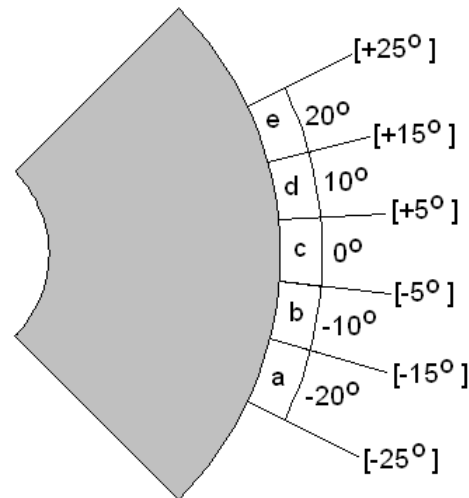


Figure 8. Magnetization directions for radially-oriented permanent magnets.

3.6. Simulation of rotor movement

There are basically two techniques for simulating the rotor movement, namely material re-identification and mesh deformation. Material re-identification has the advantage of providing solutions based on a single mesh. Discretization errors associated with different solutions are more likely to be of similar magnitude - and sign -, if a single mesh is used.

Mesh deformation or mesh distortion may be readily implemented by a parametric transformation applied to all the regions that constitute the part to be distorted. In most of the modern field simulation programs, when mesh deformation is implemented to rotate the regions that constitute the rotor, the magnetization direction of existing permanent magnets are automatically changed according the angle of rotation [17]. Consider, for example, the model shown in Fig 8. If a rotation of one degree in the counter-clockwise direction is implemented, the magnetization directions of the five sectors *a*, *b*, *c*, *d* and *e* become -19° , -9° , $+1^\circ$, $+11^\circ$ and $+21^\circ$, respectively.

4. COGGING TORQUE CALCULATIONS

4.1. Theoretical background

Produced by the distorted harmonic contents of the armature magnetomotive force, commutation torques or torque ripples are defined as torque variations due to armature current commutation and/or winding geometry. The cogging torque, on the other hand, is defined as the non-uniform torque that arises when the armature current is absent and only the excitation field is present. Therefore, the cogging torque is a function of the rotor position. Conceptually, ripple torque may exist even when cogging torque is absent, and vice versa.

In *dc* permanent-magnet motors, the interaction between the lateral edges of the magnets and the stator teeth, situated on the opposite sides of the air-gap, causes alternate cycles of restoring and anti-restoring torques as the rotor moves. When the rotor is at rest, at any position of stable equilibrium, a restoring torque arises in response to an externally applied torque trying to move it away from such a position. Once this resistance to motion is overcome, the rotor turns and accelerates, passing through an unstable equilibrium point, towards the next stable position, where a new detent torque is developed. The stable and unstable equilibrium points of a given motor are dependent on the relative geometric arrangement of the teeth - or slots opening - and magnets' pole pieces. The equilibrium points occur at positions where the net torque is zero due to the symmetry of magnetic field emerging or entering the magnets. These positions can easily be identified in machines containing an even number of slots, like the test motor under discussion in the present work.

4.2. Tests and results

Thirty six parallel-sided shaped slots form the stator of the test motor [19]. Each magnet arc spans 50 mechanical degrees and there are nine slots per pole. The distance between the centers of two adjacent slots – called slot pitch – is 10 mechanical degrees and the cogging torque characteristic is expected to be periodic, with a period of 10 mechanical degrees.

The cogging torque characteristic of the test motor has been determined numerically using the suite of finite-element programs *FEMM* [17]. Rotor movement has been simulated using the technique of mesh distortion. Torque values have been computed from field solutions related to 21 rotor positions separated by 0.5 mechanical degree. This positional displacement represents 5% of the periodic characteristic. All torque computations have been performed using the method of weighted Maxwell stress tensor [20]. The characteristic that represents the variation of the cogging torque with respect to the angular position of the rotor is exhibited in the graph of figure 9.

Observation of the graph presented in figure 9 shows that the cogging torque characteristic is in accordance with physical understanding of the device under analysis. The torque characteristic is periodic, and its period is equal to 10 mechanical degrees, exactly equal to one slot pitch. Peak torque values are of the order of 2.2 newton-metre, and this is consistent with the expected range of cogging torques in small permanent-magnet machines.

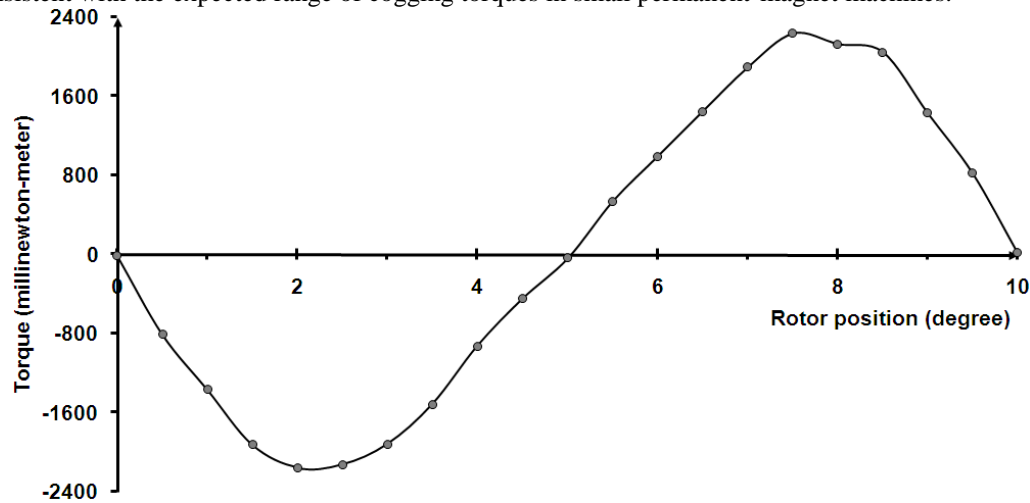


Figure 9. Cogging torque characteristic for the test motor.

5. CONCLUSIONS

Modern electromagnetic CAD systems incorporate pre- and post-processors, and their operation usually require user's interaction in both interactive and batch modes. The modeling of the problem normally involves a number of issues related to the geometry of the device under consideration and the expected characteristics of the electromagnetic fields. The planning of the numerical model may be seen as a relevant step, even for the choice of the appropriate solver, its sequence of solutions and corresponding convergence criteria. The main contribution of the present work is the presentation of a series of recommendations towards more practical and economical modeling tasks of electric machines.

6. ACKNOWLEDGEMENT

The present work is part of project number 3239/2012 of the State University of Santa Catarina. The research group acknowledges the financial support, in the form of scholarships, from the Brazilian National Council of Technological and Scientific Development (CNPq). Thanks are given to David Meeker (dmeeker@ieee.org) for the use of the finite element CAD system *FEMM*. Thanks are also due to the Brazilian Federal Agency for Postgraduate Studies (CAPES), for the sponsored access to several scientific web sites.

7. REFERENCES

- [1] K. Hameyer et al., “The art of modelling electrical machines”, *International Compumag Society Newsletter*, vol. 19, no. 2, 2012.
- [2] P. Di Barba, *Multiobjective shape design in electricity and magnetism*, Springer-Verlag, New York, 2010.
- [3] A.F. Licario-Nogueira, *Computation of cogging torques in permanent-magnet machines using the finite element method*, PhD dissertation, University of Wales, Cardiff, 1993.
- [4] Chun-Yu Hsiao, Sheng-Nian Yeh, Jonq-Chin Hwang, “A novel cogging torque simulation method for permanent-magnet synchronous machines”, *Energies*, doi: 10.3390/en4122166, vol. 4, no. 12, pp. 2166-2179, 2011.
- [5] D. Wang, X. Wang, Sang-Young Jung, “Reduction on cogging torque in flux-switching permanent magnet machine by teeth notching schemes”, *IEEE Transactions on Magnetics*, doi: 10.1109/TMAG.2012.2200237, vol. 48, no. 11, pp. 4228-4231, 2012.
- [6] Q. Chen, H. Shu, L. Chen, “Simulation analysis of cogging torque of permanent magnet synchronous motor for electric vehicle”, *Journal of Mechanical Science and Technology*, doi: 10.1007/S12206-012-0903-8, vol. 26, no. 12, pp. 4065-4071, 2012.
- [7] Jang-Young Choi and Seok-Myeong Jang, “Experimental verification and analytical approach to cogging torque calculation and reduction of permanent magnet generators with multipole rotor for wind power applications”, *Journal of Applied Physics*, vol. 103, no. 7, 2008.
- [8] C.C. Hwang, M.H. Wu, S.P. Cheng, “Influence of pole and slot combinations on cogging torque in fractional slot PM motors”, *Journal of Magnetism and Magnetic Materials*, doi: 10.1016/j.jmmm.2006.01.207, 2006.
- [9] W. Fei, P.C.K. Luk, “A new technique of cogging torque suppression in direct-drive permanent-magnet brushless machines”, *IEEE Transactions on Industry Applications*, doi: 10.1109/TIA.2010.2049551, 2010.
- [10] K. Abbaszadeh, F. Rezaee Alam, S.A. Saied, “Cogging torque optimization in surface-mounted permanent-magnet motors by using design of experiment”, *Energy conversion and Management*, doi: 10.1016/j.enconman.2011.04.009, 2011.
- [11] J.A. Wagner, “Numerical analysis of cogging torque in a brushless dc motor”, *IEEE Industry Applications Society Conference Record*, vol. CHO 999-31A, pp. 669-674, 1975.
- [12] Jae-Boo Eom, Sang-Moon Hwang, Tae-Jong Kim, Weui-Bong Jeong, Beom-Soo Kang, “Minimization of cogging torque in permanent magnet motors by teeth pairing and magnet arc design using genetic algorithm”, *Journal of Magnetism and Magnetic Materials*, 226-230, pp. 1229-1231, 2001.
- [13] L. Zhu, S.Z. Jiang, Z.Q. Zhu, C.C. Chan, “Analytical methods for minimizing cogging torque in permanent-magnet machines”, *IEEE Transactions on Magnetics*, doi: 10.1109/TMAG.2008.2011363, 2009.
- [14] A.F. Licarião Nogueira, “Performance analysis of the method of mean and difference potentials for magnetic force calculation: a technique that combines the principles of virtual work and superposition”, *International Journal of Research and Reviews in Applied Sciences*, vol. 11, no. 2, pp. 202-213, May 2012. Available: http://www.arpapress.com/Volumes/Vol11Issue2/IJRRAS_11_2_04.pdf
- [15] E.S. Hamdi, A.F. Licario-Nogueira and P.P. Silvester, “Torque computation by mean and difference potentials”, *IEE Proceedings-A*, **140**(2): 151-154, 1993.
- [16] D.A. Lowther and P.P. Silvester, *Computer-aided design in magnetics*, Springer-Verlag, New York, 1986, pp. 142.
- [17] D. Meeker, *Finite element method magnetics, user's manual*, 2010. Available: <http://femm.foster-miller.net/wiki/HomePage>
- [18] D. Meeker, *Radial Magnetization*, Available: <http://www.femm.info/wiki/RadialMagnetization>
- [19] M.G. Say, *Alternating current machines*, Longman Scientific & Technical, Essex, 1983, pp. 53.
- [20] S. McFee, J.P. Webb and D.A. Lowther, “A tunable volume integration formulation for force calculation in finite-element based computational magnetostatics”, *IEEE Transactions on Magnetics*, **24**(1): 439-442, 1988.